Study and Application of a Linear Frequency −Thickness Relation for Surface-Initiated Atom Transfer Radical Polymerization in a Quartz Crystal Microbalance

ARTICLE *in* MACROMOLECULES · APRIL 2007

Impact Factor: 5.8 · DOI: 10.1021/ma062613n

Study and Application of a Linear Frequency−Thickness Relation for Surface-Initiated Atom Transfer Radical Polymerization in a Quartz Crystal Microbalance

Jianan He,[†] Yuanzi Wu,[†] Jia Wu,[†] Xiang Mao,[†] Long Fu,[†] Tongcheng Qian,[†] Jing Fang,[†] Chunyang Xiong,[†] Jinglin Xie,[‡] and Hongwei Ma*,[†]

Department of Biomedical Engineering, College of Engineering, and Center of Analysis and Testing, College of Chemistry and Molecular Engineering, Peking University, Beijing 100871, People's Republic of China

Received November 13, 2006; Revised Manuscript Received March 2, 2007

ABSTRACT: A linear frequency−thickness ($F-T$) relation was established for surface-initiated atom transfer radical polymerization (SI-ATRP) in a quartz crystal microbalance (QCM). This quantitative $F-T$ relation is monomer dependent but independent of polymerization rate, initiator and polymer density. With this $F-T$ relation and the online monitoring capacity, QCM was successfully applied to study the kinetics of SI-ATRP mechanisms. QCM was also demonstrated to be useful in controlling film thickness at the angstrom level, which is critical in nanofabrication.

Introduction

The development of surface-initiated polymerization (SIP) has generated many new opportunities in both science and technology.[1−5] The conformation of tethered polymer chains depends on the grafting density.[5,6] As a "grafting from" strategy, SIP experiences less concentration barrier than the traditional "grafting to" strategy, such that denser films can be prepared to study interesting behaviors associated with higher grafting density (>0.06 chain nm^{-2}).[5] Controlled polymerization mechanisms in SIP format,[2] for example surface-initiated atom transfer radical polymerization (SI-ATRP), are especially important since they allow us to finely control many aspects of resulting polymers, such as film thickness and density, composition (i.e., block polymers), and functionalities. For example, block copolymers have been prepared by sequential carbocationic polymerization and SI-ATRP and found to form nanopatterns and undergo contact angle change upon exposure to different solvents.[7] Besides the scientific importance, those novel polymeric coatings from SIP are also technically significant in a wide range of applications, such as etching resistant,[8,9] colloid stabilization,[10,11] biosensors and biomaterials,[12−15] and nano-/microfabrication.[16−18]

Among many reports, very few studies have tried to kinetically understand SI-ATRP, mainly due to the lack of proper tools for kinetic studies. This analytical challenge hinders the further development of SIP.[5,21] The progress of SI-ATRP is normally monitored offline through ex-situ characterization (i.e., by ellipsometry[12,19] and X-ray photoelectron spectroscopy[15]) or arguably by adding free initiator into solution and using solution polymerization as an approximation for SIP.[5,20] Kinetic studies of SIP can be better done if one can monitor the growth of film in real time. Recently, quartz crystal microbalance (QCM) has been proposed to online monitor SI-ATRP.[22,23]

QCM has been widely used to monitor film deposition in coating instrument under vacuum condition. This is because the increase of film thickness can be calculated from the frequency change of a quartz crystal in real time based on a simple Sauerbrey equation:

$$\Delta\text{mass} = C\frac{-\Delta F}{n} \tag{1}$$

where n is the overtone number, constant C is 17.7 ng cm^{-2} for an AT-cut, 5 MHz crystal, and Δmass is the area averaged mass (ng cm^{-2}; by convention, the term "mass" was frequently used to replace the term "area averaged mass" in QCM). This equation is deduced theoretically assuming the added film has negligible viscoelastic contribution to oscillation and is small in mass compared to the crystal.[24] Operating QCM in solution has also been realized,[25] but quantitative analysis is difficult, especially for viscoelastic materials.[24,26] This is because in liquid environment the measured mass is a combination of deposited mass, entrapped solvent, and other factors such as the change of viscoelasticity of added materials.[24] For this inability of QCM to unequivocally discriminate between mass- and viscoelasticity-induced changes, previous reports obtained a curve of frequency decrease but were unable to give quantitative interpretations.[22,23] A critical component for quantitatively understanding the kinetics of SI-ATRP—how to convert the frequency change to thickness/mass change—was still missing.

Herein, we report the discovery of a simple linear relation between the change of frequency and dry thickness as a result of film growth via SI-ATRP. Variables such as monomers, polymer density, and polymerization rate were found to affect differently this frequency−thickness ($F-T$) relation. On the basis of this quantitative $F-T$ relation, we were able to directly convert frequency change of a quartz crystal to dry film thickness increase and further to quantitatively study the kinetics of SI-ATRP.

Experimental Section

The initiator thiol (ω-mercaptoundecyl bromoisobutyrate) and QCM chips were received from HZDW (Hangzhou, China) as gifts. Monomers, oligo(ethylene glycol) methyl methacrylate (OEGMA), methyl methacrylate (MMA), and ethyl methacrylate (EMA) were purchased from Aldrich.

* Corresponding author: Ph/Fax +86 10 62767142; e-mail hongwei@coe.pku.edu.cn.
[†] College of Engineering.
[‡] College of Chemistry and Molecular Engineering.

10.1021/ma062613n CCC: $37.00
Published on Web 04/04/2007

Scheme 1. A QCM Operating in Liquid Environment Was Coupled to a SI-ATRP Reactor (Optional) for Real-Time Monitoring and Controlling Film Growth

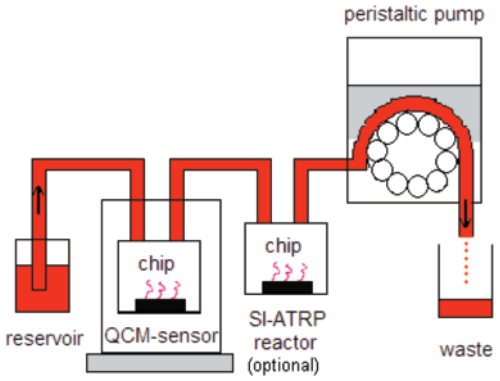

SI-ATRP in QCM. Monomers were first passed through an aluminum oxide column to remove inhibitors. All QCM chips (gold-coated quartz crystals) were first cleaned in an UV/ozone Tip-Cleaner (BioForce Nanosciences, Ames, IA) and used immediately for the preparation of self-assembled monolayers (SAMs) of initiator as reported.[23] A binary mixed SAM that consisted of the initiator (I) and undecanethiol (U) was prepared as reported.[19] Undecanethiol was used as a dilutent to vary the density of initiator. QCM chips were immersed into ethanol solutions of different U/I ratio for overnight, resulting in QCM chips coated with mixed SAMs. The initiator-modified QCM chip was then placed in a Q-Sense E4 sensor (Q-Sense, Gothenburg, Sweden). The overall reaction system is illustrated in Scheme 1. From left to right, reaction solutions were kept under nitrogen and linked to a QCM sensor chamber. E4 was then connected to a SI-ATRP reactor (optional), which was used to demonstrate the online monitoring ability of QCM. Reaction solution was pumped through E4 by a peristaltic pump. Two different types of SI-ATRP were conducted, namely regular and activator generated by electron transfer[27] (AGET) SI-ATRP.

Regular SI-ATRP. Monomer MMA, EMA, and OEGMA526 (M_w = 526) were polymerized under the following conditions. After assembly, the E4 system was first purged with nitrogen for 25 min (deoxygenated). Meanwhile, incomplete reaction mixture (IRM) and complete reaction mixture (CRM) were prepared: IRM was obtained by mixing well with water (3 mL), methanol (12 mL), and the monomer; CRM was obtained by adding the catalyst, CuBr (~36 mg, 0.25 mmol) and bipyridine (~78 mg, 0.5 mmol), to the IRM, resulting in a dark-red solution. The mole ratio of monomer/Cu^+ was 60:1 (MMA), 70:1 (EMA), and 40:1 (OEGMA526). Both IRM and CRM were deoxygenated right before use. The reaction system was also first deoxygenated and then primed with IRM until a stable baseline was established. Polymerization was initiated by pumping the CRM mixture to the sensor cell at a speed of 70 mL h^{-1} (1−2 min) and reduced to ~3 mL h^{-1} after complete exchange of IRM with CRM (indicated by color change, from colorless to red). SIP was continued for a specified time (30−360 min) at ~25 °C and monitored by QCM in real time. The polymerization was stopped by replacing CRM with IRM and rinsed with IRM until a stable baseline reached. Samples were finally pulled out of the sensor cell and rinsed with methanol and Milli-Q water and dried under flowing nitrogen before ellipsometry measurement.

AGET SI-ATRP. Monomer OEGMA300 and OEGMA475 were polymerized under the following conditions. IRM was deoxygenated Milli-Q water. CRM was prepared by mixing well two parts. Part 1 was a transparent, pale-blue solution, prepared by adding a specified amount of $CuCl_2$/Bipy (1:2 mole ratio) and a fixed amount monomer to 5 mL of Milli-Q water. Part 2 was a colorless solution, prepared by adding a specified amount of ascorbic acid (AscA) to 5 mL of Milli-Q water. After both solutions were deoxygenated, two parts were mixed together under nitrogen protection. The mixture was further deoxygenated, and the resulting CRM was red in color due to the reduction of deactivator Cu^{2+}/Bipy complex to activator Cu^+/Bipy complex. The resulting mixture had a mole ratio of monomer:$CuCl_2$/Bipy/AscA = 200/1/2/1, with a feed [$CuCl_2$] of 2.76 mM. Running experiment in QCM was the same as regular SI-ATRP described above.

Ellipsometry. Film thickness was measured on a M-2000V spectroscopic ellipsometer (J.A. Woollam Co., Inc.) at angles of 65°, 70°, and 75° and wavelengths from 400 to 800 nm. Ellipsometric data were fitted for the thickness with material-specific models, i.e., SAMs and poly(OEGMA) films with fixed (An, Bn) values of (1.45, 0.01) and (1.46, 0.01), respectively, using a Cauchy layer model;[12] PMMA and PEMA were fitted with a model provided by the manufacturer. The ellipsometric thickness for each sample was independently measured at three different locations and is reported as the average ± standard error.

X-ray Photoelectron Spectroscopy. XPS (AXIS Ultra by Kratos Analytical, UK) was used to determine the surface density of initiator of mixed SAMs. Monochromatic Al Kα X-rays (1486.7 eV) were employed. The X-ray source was 2 mm nominal X-ray spot size operating at 15 kV, 8.9 mA for both survey and high-resolution spectra. Survey spectra, from 0 to 1200 eV binding energy (BE), were recorded at 160 eV pass energy with an energy step of 1.0 eV and a dwell time of 100 ms. High-resolution spectra were recorded at 20 eV pass energy with an energy step of 0.1 eV and a dwell time of 1.2 s, with a typical average of 12 scans. The operating pressure of the spectrometer was typically ~10^{-9} mbar. For quantitative XPS measurements, a survey scan was first taken at an angle of 90°, defined as the angle between the collection axis of photoelectron analyzer and sample plane. High-resolution scans for C 1s and Au 4f were then taken at angle the of 35°. All peaks were referenced to Au 4f at 84.0 eV in the survey scan spectra and to the CH_x component at 285.0 eV in the deconvoluted high-resolution C 1s spectra. Oxygen was detected from the SAM of undecanthiol (0.6 at. % from survey scan), which could be attributed to impurities in undecanethiol (98% purity from Aldrich) and the oxidation of adsorbed thiols. For χ_I^{Sur} determination, the measured atomic percent oxygen of mixed SAMs of initiator and undecanethiol were corrected for this baseline oxygen level. Details of calculation have been published elsewhere.[19] All data were collected and analyzed using software provided by the manufacturer.

Mathematical Analysis. The moving window average method[29] is used to smooth the QCM curves, and then the curve of polymerization rate is obtained by applying a numerical differential[30] to each smoothed curve.

Results and Discussion

QCM Curve Reflects the Kinetics of SI-ATRP. The experimental setup is illustrated in Scheme 1 (see details in Experimental Section). A typical run of regular SI-ATRP was conducted as follows: an initiator-modified QCM chip was mounted in a sensor chamber, primed with incomplete reaction mixture (IRM) until a stable baseline was established (Figure 1, from 0 to 10 min). Polymerization was initiated by pumping the complete reaction mixture (CRM) through the sensor cell. SI-ATRP was continued for ~120 min at ~25 °C and monitored by QCM in real time (Figure 1, from 10 to 130 min). To quench polymerization, CRM was replaced by IRM, and an end-baseline was established by rinsing with IRM for ~20 min (Figure 1, from 130 to 150 min). Samples were then pulled out from the sensor cell and rinsed thoroughly with methanol and Milli-Q water and then dried under flowing nitrogen for thickness measurement by ellipsometry.

Figure 1 was a typical QCM curve for SI-ATRP of OEGMA526. At ~10 min point, frequency decrease was mainly attributed to the instantaneous initiation of polymer growth upon the replacement of IRM with CRM. After this initial period, one observed a continuous decrease of frequency as a result of polymer growth. When the CRM was replaced with IRM, frequency quickly reached a stable state, indicating a complete stop of polymer growth and zero desorption of tethered polymer

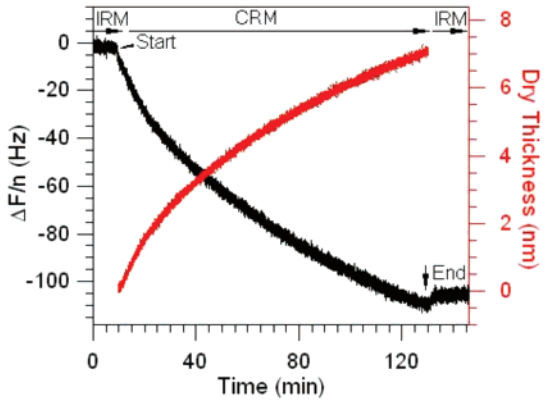

Figure 1. The black curve is a typical QCM curve of SI-ATRP. Polymerization was initiated by replacing IRM with CRM. The change in frequency ($n = 3$) of a quartz crystal was recorded in real time and can be converted to a thickness curve (the red curve) using a k value (0.0703 for OEGMA526) from Table 1.

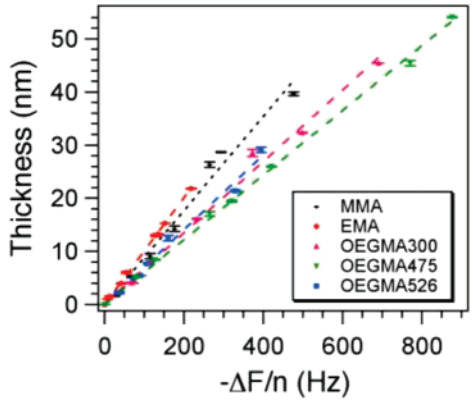

Figure 2. The final frequency change and thickness change obey a simple linear relation for a number of monomers within the range from 0 to 55 nm. See k values in Table 1. All fitting have a R^2 value of ~0.99.

chains. The final change of frequency ($\Delta F/n$, $n = 3$ is the overtone number) was the difference between the two baselines.

In order to reveal the relation between frequency change and thickness increase, a set of polymerizations were conducted for monomer OEGMA526. These experiments were identical except the duration of polymerization (from 30 to 360 min). Each run used a new QCM chip and the resulting polymeric film was measured for dry ellipsometric thickness. By plotting the dry film thickness against $\Delta F/n$, as indicated in Figure 2, one found a simple linear fitting could be applied, expressed as eq 2:

$$\text{thickness} = k\frac{-\Delta F}{n} \tag{2}$$

where n is the overtone number ($n = 3$ in this paper) and the thickness was measured by ellipsometry at air−solid mode. The formula $y = ax + b$ was not used because we believed eq 2 was more physically realistic: zero thickness at zero time (no polymerization).

Given the real-time nature of the QCM curve, this quantitative $F-T$ relation established the foundation for kinetic analysis: for each SI-ATRP in QCM, the rate of frequency decrease, $d(-\Delta F/n)/dt$, reflected the rate of dry thickness increase (i.e., the polymerization rate). Thus, to apply QCM for kinetic study of SI-ATRP, the key question is then the generality of this quantitative $F-T$ relation: whether the k in eq 2 is a function of the polymerization conditions, i.e., monomer used, polymer and initiator density, and catalyst systems (polymerization rate).

***k* Is Monomer Dependent.** Monomer OEGMA526 was chosen as it had demonstrated applications and the performance of resulting poly(OEGMA) films depended heavily on the film thickness.[12,13] In order to confirm that this empirical equation is applicable to other monomers, we further tested MMA, EMA, OEGMA300, and OEGMA475 (Table 1). MMA is an extensively studied model monomer,[4,30] and PMMA is also widely used in photolithography as a photoresist material.[9] Other monomers were chosen for their structural similarity to MMA or OEGMA526. The influence of monomer property on $F-T$ relation was clearly revealed in Figure 2 and Table 1.

Vinyl group functionalized monomer was chosen because the ATRP mechanism works best for vinyl monomers.[31] MMA, EMA, and OEGMA were polymerized under similar conditions: 1/4 H_2O/methanol as the solvent and CuBr/Bipy complex as the catalyst ([CuBr] at 0.017 M). From Table 1, the k value increased from MMA to EMA as the molecular weight increased. Interestingly, OEGMA526 had a lower k compared with MMA and EMA although it had the highest molecular weight, implying that the structure of resulting polymer has great influence on the k value. For OEGMA family, the k value did not obey this simple trend of linear increase: OEGMA475 had the lowest k value of 0.0609, but OEGMA300 and OEGMA526 had a similar k value at ~0.07. One obvious structural difference between PMMA/PEMA and poly(OEGMA) was the "bottlebrush" shape of poly(OEGMA). These two families of polymers were also different in their solubility in water: PMMA/PEMA were hydrophobic polymers, and poly(OEGMA) were amphiphilic polymers (hydrophobic MMA backbones and hydrophilic OEG pendent chains). We hypothesized that the size of pendent chain of OEGMA may lead to a minimal k at 9 ethylene glycol (CH_2CH_2O) repeat units. A systematic testing of more monomers will help us to understand the k dependence on the nature of monomers, which includes the structure of monomer and resulting polymer, solubility and viscoelasticity in the reaction solution, molecular weight, etc.

The working range (linear range, <55 nm, monomer dependent) was limited by the polymerization system used here. Previous reports have identified a level-out thickness of ~40 and ~50 nm for OEGMA475[13,19] and MMA,[30] respectively. To check the working range limited by the QCM would require different polymerization systems that are able to break the thickness limitation. For example, thicker films of OEGMA300 and OEGMA475 were polymerized using AGET system (see below).

On the basis of this simple linear relation, the QCM curve was converted to a film-growth curve (Figure 1, the red curve). We emphasize here that this linear $F-T$ relation does not implicate a linear film growth. In fact, the film growth (i.e., polymerization rate) was not linear with time, as clearly indicated by the QCM curve (Figure 1).

***k* Is Independent of Polymer and Initiator Density.** In SI-ATRP, simultaneous chain growth is ensured through a simultaneous initiation and a fast activation−deactivation process.[31] However, Matyjaszewski et al. found that there was differentiated chain growth in SI-ATRP: the number of growing chains decreases gradually as the film thickness increases,[21] which prevents the formation of films with high density, uniform chain length, and unlimited thickness. The existence of differentiated chain growth implicates the k value may be independent of polymer density.

Resumptive polymerization was commonly used to examine if the polymerization mechanism is living.[32] We carried out resumptive polymerizations to prove SI-ATRP is a controlled/

Table 1. *k* Value Depends on the Nature of Monomers

vinyl monomer	$(CH_2{=}C)CH_3CO{-}R$	M_w[a]	ATRP condition[b]	k[c]
MMA	$-OCH_3$	100	regular SI-ATRP	0.0884
EMA	$-OCH_2CH_3$	114	regular SI-ATRP	0.1002
OEGMA 300	$-O(CH_2CH_2O)_6CH_3$	300	AGET SI-ATRP	0.0673
OEGMA 475	$-O(CH_2CH_2O)_9CH_3$	475	AGET SI-ATRP	0.0609
OEGMA 526	$-O(CH_2CH_2O)_{10}OH$	526	regular SI-ATRP	0.0703

[a] M_n for OEGMAs. [b] 25 °C for all experiments; see Experimental Section for monomer/Cu^+ ratio. [c] $R^2 \sim 0.99$ for all fittings.

living mechanism. For a QCM chip, the first run of SI-ATRP of OEGMA300 was conducted as normal and measured for its ellipsometric thickness, resulting in the first data point (32.4 nm thickness increase with 456 Hz frequency decrease, the ratio of thickness/time $k = 0.0711$). This chip was then immediately used for a second run of SI-ATRP, resulting in the second data point (2.5 nm increase with 43 Hz decrease, $k = 0.0581$). The success of the second run confirmed that the polymerization mechanism was living. However, we believed that some of the growing sites were damaged, and hence the number of total growing sites was reduced during the exchange process (from CRM to IRM) as well as after exposure to air at the end of the first run of SI-ATRP. The same experiments were also conducted for MMA, EMA, and OEGMA526 (data not shown). A relatively thicker film was easily prepared after the first run. The second run, however, quickly reached a state where the frequency decrease was less than 1 Hz min^{-1} as monitored by QCM. We attributed this slow polymerization rate to the reduced number of initiating sites. Therefore, the density of polymer chain will be different for the first and second runs. Interestingly, the two k values for the resumptive polymerization of OEGMA300 were comparable to the k value in Table 1 (0.0673, not fitted from the resumptive polymerization data), which strongly implicated that the k ($F-T$ relation) might be independent of polymer density.

For more direct evidence, we applied the mixed SAM technique[33] to systematically change the surface density of initiators on the QCM chip. Previous studies have demonstrated that the polymer density can be controlled by varying the surface density of initiator.[19,34,35] A binary system was used: initiator thiol and undecanethiol (U) were dissolved into ethanol (for nine different ratios), where U was used as a dilutent to vary the initiator (I) density. QCM chips were immersed into ethanol solutions overnight, resulting in mixed SAMs coated QCM chips (i.e., varied initiator density). XPS was used to calibrate the final surface density of initiator ($\chi_I^{Sur} = M_I/(M_I + M_U)$, where M is the number of molecules[19]), corresponding to the solution ratio of initiator (χ_1^{Sol}, Figure 3A). Those mixed SAMs with varied initiator density was then processed for SI-ATRP of OEGMA475 in QCM-D as aforementioned. The $F-T$ relation was constructed in Figure 3B: the dashed line was from eq 2 using an OEGMA475 specific k value of 0.0609. Since no data from mixed SAMs was used to fit this k value and all $F-T$ pairs from mixed SAMs agreed well with this dashed line, we believe the k value was independent of the initiator and polymer density.

***k* Is Independent of Polymerization Rate and Useful in Kinetic Studies.** It is clear from Figure 1 that the rate of film growth was not linear; therefore, we expect that the data in Figure 2 were obtained under different polymerization rate, indicating variation in the rate of polymerization has no or negligible influence on the k value. To validate this hypothesis, in this section, the polymerization rate was intentionally varied by using different catalyst systems (Table 2), namely, activator generated by electron transfer (AGET) systems. In AGET ATRP, the oxidatively stable $CuCl_2$/bipyridine complex (deactivator) was used at the beginning, and this deactivator was reduced in situ to the activator form, CuCl/Bipy complex, by reducing agent such as ascorbic acid (AscA). Although there is no report on AGET SI-ATRP yet, this improvement of solution ATRP is apparently applicable to SI-ATRP. AGET is comparable with regular ATRP where both Cu^+ and Cu^{2+} were added since the amount (in moles) of Cu^{2+} is greater than that of AscA. However, regular SI-ATRP in the methanol/water mixture

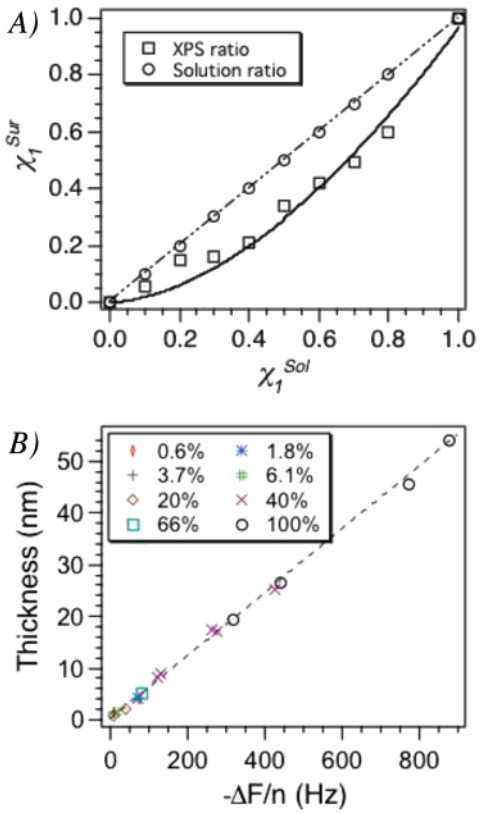

Figure 3. The linear $F-T$ relation is independent of initiator and polymer density. (A) XPS surface density of initiator on mixed SAMs. (B) Dashed line was from eq 2 using the monomer specific k value. Data ($F-T$) from mixed SAMs agreed well with data from initiator SAMs; listed are the XPS surface density of initiator.

Table 2. Polymerization Rate Was Varied by the Ratio of Monomer/Catalyst

entry[a]	OEGMA 475/Cu^{2+}/AscA[b]	[Bipy] (mM)[c]	$d(-\Delta F/n)/dt$ (Hz/s)[d]
1	200/1/0.7	5.46	0.092
2	200/0.5/0.7	2.86	0.263
3	200/0.2/0.7	1.17	0.500
4	200/0.1/0.7	0.06	0.610
5	200/0.01/0.7	0.06	0.733

[a] For all reactions, [OEGMA475] = ~0.6 M. [b] The mole feed ratio of OEGMA475, Cu^{2+}, and AscA. Note the feed ratio is not the final ratio, nor are the final concentrations of Cu^{2+} and AscA known. [c] For all reactions except entry 5, the mole feed ratio of Cu^{2+}/Bipy is 1/2. [d] The rate of frequency decrease was estimated after 10 min of initiation (for a period of 10 min).

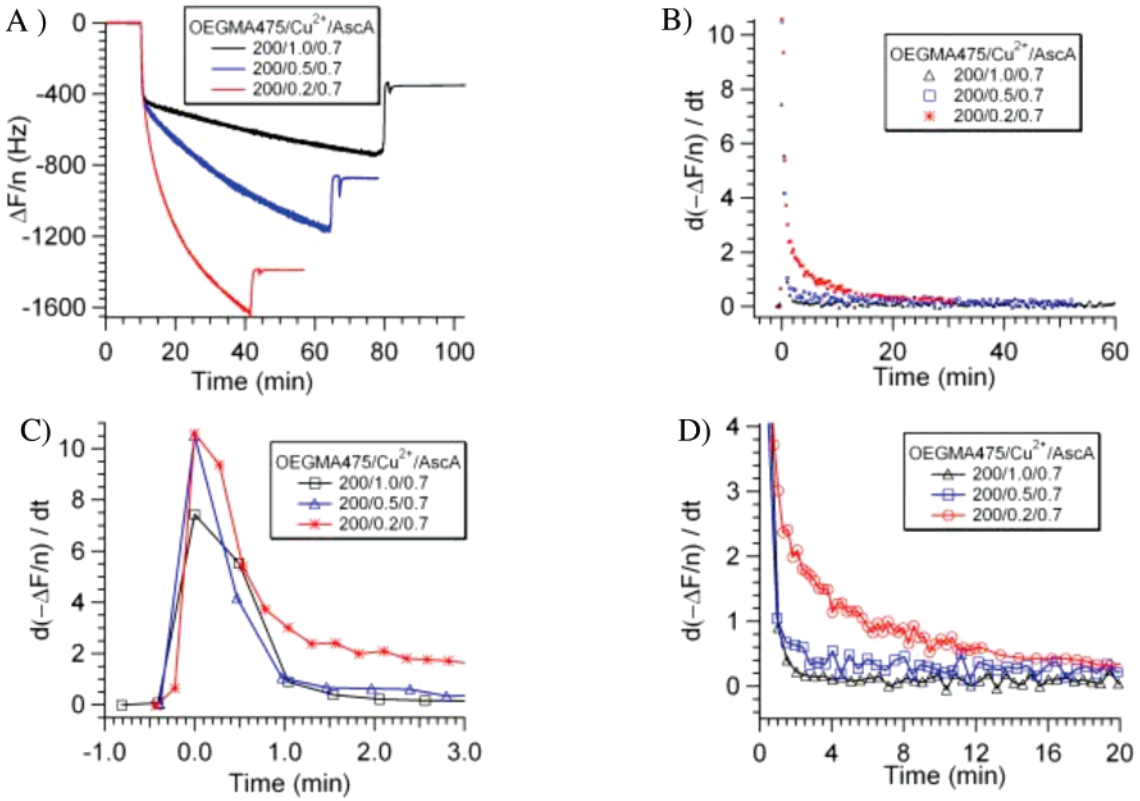

Figure 4. (A) Three representative QCM curves of different [Cu^{2+}]. (B) Differential of the QCM curve gives the rate of polymerization (Hz/s). (C) Enlarged area is the first 3 min (lines connected between dots are only as a guide to the eyes). The peaks were due to solution-induced frequency change. (D) Enlarged area of the first 20 min (lines connected between dots are only as a guide to the eyes). The gradual decrease of polymerization rate supported the idea of differentiated chain growth.

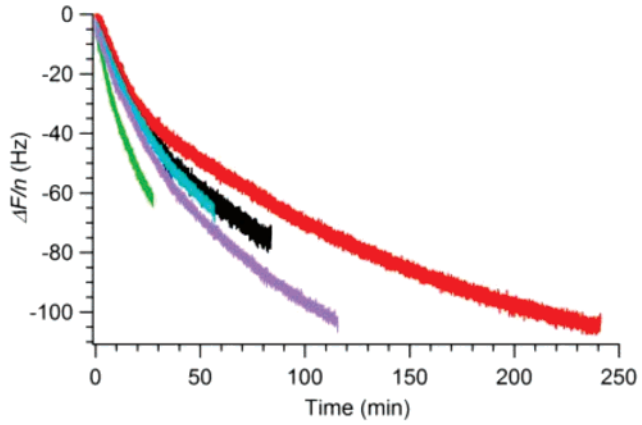

Figure 5. Reproducing regular SI-ATRP is difficult: (A) QCM curves of five identical runs (except reaction time) indicated poor reproducibility of regular SI-ATRP, mainly due to the oxygen sensitive nature of the catalyst used (Cu^{+}). Such difference is clear in QCM curves but most likely considered as variations and averaged in batch mode experiments.

proceeds in a controlled fashion even without adding Cu^{2+} at the beginning.[12]

Three representative QCM curves of AGET SI-ATRP (entries 1−3 of Table 2) were plotted in Figure 4A for comparison. All reactions were conducted as described above, except the IRM here was deoxygenated Milli-Q water only and no monomer was added. This difference in these two IRMs led to a dramatic difference in the QCM curves (see below). Although the QCM curves were different in Figures 1 and 5, the final value of $\Delta F/n$ was calculated in the same way, which was the difference between the two baselines. We found the same $F-T$ relation (i.e., the same k value) for the five runs of AGET SI-ATRP from Table 2 (Figure 2, green curve). Thus, the k value of eq 2 is independent of polymerization rate. To summarize, we demonstrated a quantitative $F-T$ relation that was monomer dependent but independent of polymer density and polymerization rate. We applied this quantitative $F-T$ relation to study the kinetics of AGET SI-ATRP.

In a previous report,[23] we tested the influence of viscosity on frequency change using undecanethiol-modified QCM chips (no polymerization will be initiated from such chips) and confirmed that differences in viscosity alone will introduce an immediate large frequency change and quickly reach a steady state. For IRM with monomer (Figure 1), when the IRM was replaced with CRM, there was no immediate significant decrease in frequency because the viscosities of IRM and CRM were similar. The recorded gradual decrease of frequency was due to polymerization. For IRM without monomer (Figure 4), we observed an immediate significant decrease in frequency when the IRM was replaced with CRM, typically lasting for ~1 min. This dramatic frequency change was mainly attributed to the change of viscosity upon switching from IRM to CRM (~400 Hz as estimated from Figure 4) and with a small portion of contribution from polymerization (less than 20 Hz as estimated from Figure 1). The black curve in Figure 4 was a typical case, which had a turning point indicating the influence from viscosity diminished completely. After this turning point, the observed frequency decrease was due solely to the continuous polymer growth. For the blue and red curves, such a turning point was not obvious but can be identified by numerical differential (see below).

The concentration of monomer was constant (OEGMA475, ~0.6 M) because the consumption of monomer was negligible for SI-ATRP in QCM under flow condition. The feed [AscA]

was kept constant and the feed [Cu^{2+}] was varied (from 2.76 to 0.03 mM). For a semiquantitative analysis, the rate of polymerization was first roughly estimated by linearly fitting a 10 min period of a QCM curve after 10 min of initiation. We noticed that the rate of polymerization varied nonlinearly as the feed [Cu^{2+}] changed. Advanced mathematical analysis is shown in Figure 4B−D.

In Figure 4A, three representative QCM curves (entries 1−3 of Table 2) were plotted for comparison. Polymerization was stopped when the rate of frequency decrease was close to 1 Hz/min (0.016 Hz/s). Figure 4B was obtained by applying numerical differential[29] to the three QCM curves in Figure 4A, which gave the rate of polymerization ($d(-\Delta F/n)/dt$, Hz/s) as a function of time (min). As previously discussed, the initial high value of $d(-\Delta F/n)/dt$ was mainly due to the exchange of solution (from IRM to CRM) and was overlapped with the polymer growth. This trend was clear for the black curve in Figure 4A but was difficult to identify for the blue and red curves. However, after applying numerical differential, a peak was visualized in Figure 4C (enlarged area of the first 3 min in Figure 4B). Since the black curve had a nearly constant polymerization rate, one can roughly estimate the rate of frequency change induced by viscosity change at 7.5 Hz/s. The red curve had the same viscosity-induced frequency change but showed a higher peak value due to its higher instant polymerization rate, which could be roughly estimated to be 3 Hz/s at 1 min point.

It was clear from Figure 4D that for conditions that induced a high initial polymerization rate the duration of maintaining this high rate was very short. For the black curve, we found an almost constant $d(-\Delta F/n)/dt$ at ∼0.06 Hz/s (0.0036 nm/s), indicating a stabilized polymer growth. For the red curve, there was a continuous decrease of $d(-\Delta F/n)/dt$. We reasoned the continuous decrease of $d(-\Delta F/n)/dt$ was mainly due to the differentiated chain growth. This also partially explains why there is a cutoff thickness. Higher polymerization rate was useful in breaking the cutoff thickness limitation but only with limited success. For example, using AGET SI-ATRP, the cutoff thickness was ∼50 nm. Previously, we reported a cutoff thickness of ∼40 nm for OEGMA475.[11,12] With the real-time monitoring feature, optimizing the reaction condition of SI-ATRP using QCM would be pleasant compared with the tedious batch mode fashion.

Poly(OEGMA) was expected to be soluble in water. However, PMMA of high molecular weight was insoluble in the reaction solvent (1/4 H_2O/MeOH). Since the monomer MMA and EMA were soluble in this mixture, low molecular PMMA and PEMA might be soluble in 1/4 H_2O/MeOH mixture. For direct evidence, we carried out the following experiments: an initiator modified QCM chip was placed in a flask and processed for SI-ATRP as normal except that free initiators were introduced right after CRM was transferred into the flask. Addition of free initiators was used to proximate SI-ATRP.[5,20] Insoluble materials appeared in less than 5 min, indicating that free PMMA and PEMA from solution polymerization were insoluble in 1/4 H_2O/MeOH solvent. We also observed insoluble polymers deposited on the surface of QCM chips. Given the short polymerization time, we suspected the insoluble PMMA and PEMA were of low molecular weight. However, in SI-ATRP of MMA and EMA in QCM-D, polymerization can last for hours and polymer coatings as thick as 25 nm can be prepared. We were unable to conclude the impact of solubility of surface tethered polymers on the $F-T$ relation.

There are other variables not considered in this paper, such as the effect of temperature and solvent. These variables may lead to a different k value and limit the generalness of this $F-T$ relation. Nevertheless, we expect the k will be the same for a fixed condition, and one can obtain this k value from a limited number of experiments, for example, three runs. Even with the need of establishing a standard curve first, one can still save time in daily applications and more importantly give quantitative interpretation of frequency decrease, as demonstrated below.

QCM for Online Monitoring Film Growth. In comparison of Sauerbrey eq 1, the empirical eq 2 can be further developed to have the following form:

$$\Delta\text{mass} = \text{thickness} \times \rho = k\rho \frac{-\Delta F}{n} = K \frac{-\Delta F}{n} \qquad (3)$$

where ρ is the density of bulk polymer, K is the monomer-dependent constant, and Δmass is the area averaged mass. We assumed the tethered polymer film in its collapsed state has the same density as its bulk polymer. This assumption is also the basis for ellipsometric modeling.[19]

Unlike the Sauerbrey equation, which has a universal constant value of 17.7 ng cm^{-2}, the empirical eq 3 has a monomer-dependent constant K, 7.60 and 10.24 ng cm^{-2} for OEGMA526 ($\rho = 1.08$ g cm^{-3})[36] and MMA ($\rho = 1.19$ g cm^{-3} from Aldrich), respectively. This equation allows one to estimate the dry mass (area averaged mass) of deposited film using frequency measured in liquid environment. Extracting dry mass from QCM data has been difficult because $\Delta F/n$ is an overall measure of mass change (polymer and entrapped solvent) coupled to oscillation and mass decrease due to viscoelastic damping in an aqueous environment.[24] The wet mass obtained by either modeling or direct application of Sauerbrey equation was found in poor agreement with the mass obtained by other techniques such as ellipsometry and optical waveguide (OWLS): QCM gave a 1−3 times higher value of mass than the ellipsometry and OWLS did.[24]

The QCM curve is also advantageous in studying SIP, compared with curves constructed via batch mode methods. One is now able to follow a continuous trend of SIP through a QCM curve with a time resolution at half second, which is only limited by the sampling frequency of the microbalance. The traditional postsynthesis characterization (batch mode) requires a minimal of 10 min interval in order to obtain a decent resolution. This is a 3 orders of magnitude increase in terms of time resolution. The initial period of regular SI-ATRP is known to vary among identical experiments, especially for cases where no deactivators were added.[21] This is in agreement with our finding that the reproducibility of regular SI-ATRP was poor (Figure 5).

We attributed this variation to the fact that the catalyst system (Cu^{+}) used was oxygen sensitive and the nitrogen bubbling procedure could also change the ratio of methanol and water in reaction mixture, which is known to alter the speed of film growth,[19] plus ATRP was considered to be only a pseudo-living polymerization mechanism.[30] This leads to a serious problem for practical use of regular SI-ATRP. For example, nanodevice fabrication demands the precise control of film thickness at the nanometer level.[16,17] Without tracing film growth in real time, the manufacturer has to rely on a standard curve constructed by batch mode and stop the reaction at predetermined time. A deviation from this curve would be costly in mass production, but Figure 5 indicates the chance for such a deviation to happen is quite high. With a coupled QCM as online monitor (Scheme 1) and the quantitative $F-T$ relation, one can terminate the polymerization when a desired $\Delta F/n$ value was reached, which

guarantees accuracy at the nanometer level. Furthermore, using QCM as a online monitor, one can gain control over the uncontrolled free radical polymerization (FRP), whose reaction condition is mild and has many industrial applications.[37]

In conclusion, we discovered a quantitative frequency−thickness relation for SI-ATRP in QCM. This linear $F-T$ relation gave a k value which was dependent on monomer but independent of the polymerization rate, initiator, and polymer density. This constant k allows a quantitative understanding of the SIP kinetics, which will facilitate the further development of SIP aimed to obtain polymer brushes of novel properties. We expect that with this simple $F-T$ relation QCM operating in liquid will be as useful as QCM operated in vacuum, where quantitative control is critical.

Acknowledgment. The authors thank Dr. Yanyi Huang for helpful discussions. This work was partially supported by the NSFC grant (20644001) to H.M. and NSFC grant (10502001) to C.Y.X.

References and Notes

(1) Advincula, R. C.; Brittain, W. J.; Caster, K. C.; Ruhe, J. *Polymer Brushes: Synthesis, Characterization, Applications*; Wiley-VCH: Weinheim, 2004.
(2) Edmondson, S.; Osborne, V. L.; Huck, W. T. S. *Chem. Soc. Rev.* **2004**, *33*, 14−22.
(3) Jennings, G. K.; Brantley, E. L. *Adv. Mater.* **2004**, *16*, 1983−1994.
(4) Pyun, J.; Kowalewski, T.; Matyjaszewski, K. *Macromol. Rapid Commun.* **2003**, *24*, 1043−1059.
(5) Tsujii, Y.; Ohno, K.; Yamamoto, S.; Goto, A.; Fukuda, T. *Adv. Polym. Sci.* **2006**, *197*, 1−45.
(6) Zhao, B.; Brittain, W. J. *Prog. Polym. Sci.* **2000**, *25*, 677−710.
(7) Zhao, B.; Brittain, W. J. *Macromolecules* **2000**, *33*, 8813−8820.
(8) Jeon, N. L.; Choi, I. S.; Whitesides, G. M.; Kim, N. Y.; Laibinis, P. E.; Harada, Y.; Finnie, K. R.; Girolami, G. S.; Nuzzo, R. G. *Appl. Phys. Lett.* **1999**, *75*, 4201−4203.
(9) Zhou, F.; Liu, W. M.; Hao, J. C.; Xu, T.; Chen, M.; Xue, Q. J. *Adv. Funct. Mater.* **2003**, *13*, 938−942.
(10) Perruchot, C.; Khan, M. A.; Kamitsi, A.; Armes, S. P.; von Werne, T.; Patten, T. E. *Langmuir* **2001**, *17*, 4479−4481.
(11) Duan, H. W.; Kuang, M.; Wang, D. Y.; Kurth, D. G.; Mohwald, H. *Angew. Chem., Int. Ed.* **2005**, *44*, 1717−1720.
(12) Ma, H.; Hyun, J.; Stiller, P.; Chilkoti, A. *Adv. Mater.* **2004**, *16*, 338−341.
(13) Fan, X. W.; Lin, L. J.; Dalsin, J. L.; Messersmith, P. B. *J. Am. Chem. Soc.* **2005**, *127*, 15843−15847.
(14) Tugulu, S.; Arnold, A.; Sielaff, I.; Johnsson, K.; Klok, H. A. *Biomacromolecules* **2005**, *6*, 1602−1607.
(15) Xiao, D. Q.; Wirth, M. J. *Macromolecules* **2002**, *35*, 2919−2925.
(16) Mulvihill, M. J.; Rupert, B. L.; He, R. R.; Hochbaum, A.; Arnold, J.; Yang, P. D. *J. Am. Chem. Soc.* **2005**, *127*, 16040−16041.
(17) von Werne, T. A.; Germack, D. S.; Hagberg, E. C.; Sheares, V. V.; Hawker, C. J.; Carter, K. R. *J. Am. Chem. Soc.* **2003**, *125*, 3831−3838.
(18) Rutenberg, I. M.; Scherman, O. A.; Grubbs, R. H.; Jiang, W. R.; Garfunkel, E.; Bao, Z. *J. Am. Chem. Soc.* **2004**, *126*, 4062−4063.
(19) Ma, H.; Wells, M.; Beebe, Jr., T. P.; Chilkoti, A. *Adv. Funct. Mater.* **2005**, *16*, 640−648.
(20) Prucker, O.; Ruhe, J. *Macromolecules* **1998**, *31*, 602−613.
(21) Matyjaszewski, K.; Miller, P. J.; Shukla, N.; Immaraporn, B.; Gelman, A.; Luokala, B. B.; Siclovan, T. M.; Kickelbick, G.; Vallant, T.; Hoffmann, H.; Pakula, T. *Macromolecules* **1999**, *32*, 8716−8724.
(22) Moya, S. E.; Brown, A. A.; Azzaroni, O.; Huck, W. T. S. *Macromol. Rapid Commun.* **2005**, *26*, 1117−1121.
(23) Ma, H.; Textor, M.; Clark, L. R.; Chilkoti, A. *Biointerphases* **2006**, *1*, 35−39.
(24) Höök, F.; Vörös, J.; Rodahl, M.; Kurrat, R.; Böni, P.; Ramsden, J. J.; Textor, M.; Spencer, N. D.; Tengvall, P.; Gold, J.; Kasemo, B. *Colloids Surf. B* **2002**, *24*, 155−170.
(25) Ward, M. D.; Buttry, D. A. *Science* **1990**, *249*, 1000−1007.
(26) Rodahl, M.; Hook, F.; Krozer, A.; Brzezinski, P.; Kasemo, B. *Rev. Sci. Instrum.* **1995**, *66*, 3924−3930.
(27) Min, K.; Gao, H. F.; Matyjaszewski, K. *J. Am. Chem. Soc.* **2005**, *127*, 3825−3830.
(28) Press, W. H.; Teukolsky, S. A.; Vetterling, W. T.; Flannery, B. P. *Numerical Recipes in C, The Art of Scientific Computing*, 2nd ed.; Cambridge University Press: Cambridge, 1992.
(29) Burden, R. L.; Faires, J. D. *Numerical Analysis*, 6th ed.; Brooks-Cole Publishing Co.: Singapore, 1997.
(30) Jones, D. M.; Huck, W. T. S. *Adv. Mater.* **2001**, *13*, 1256−1259.
(31) Matyjaszewski, K.; Xia, J. H. *Chem. Rev.* **2001**, *101*, 2921−2990.
(32) Rademacher, J. T.; Baum, R.; Pallack, M. E.; Brittain, W. J.; Simonsick, W. J. *Macromolecules* **2000**, *33*, 284−288.
(33) Bain, C. D.; Evall, J.; Whitesides, G. M. *J. Am. Chem. Soc.* **1989**, *111*, 7155−7164.
(34) Jones, D. M.; Brown, A. A.; Huck, W. T. S. *Langmuir* **2002**, *18*, 1265−1269.
(35) Bao, Z. Y.; Bruening, M. L.; Baker, G. L. *Macromolecules* **2006**, *39*, 5251−5258.
(36) Sharma, S.; Johnson, R. W.; Desai, T. A. *Langmuir* **2004**, *20*, 348−356.
(37) Moad, G.; Solomon, D. H. *The Chemistry of Free Radical Polymerization*, 1st ed.; Pergamon: Tarrytown, NY, 1995.

MA062613N